RESEARCH ARTICLE

Plasticized Drug-Loaded Melt Electrospun Polymer Mats: Characterization, Thermal Degradation, and Release Kinetics

ATTILA BALOGH,[1] GÁBOR DRÁVAVÖLGYI,[1] KORNÉL FARAGÓ,[1] ATTILA FARKAS,[1] TAMÁS VIGH,[1] PÉTER LAJOS SÓTI,[1] ISTVÁN WAGNER,[1] JÁNOS MADARÁSZ,[2] HAJNALKA PATAKI,[1] GYÖRGY MAROSI,[1] AND ZSOMBOR KRISTÓF NAGY[1]

[1]Organic Chemistry and Technology Department, Budapest University of Technology and Economics, Budapest H-1111, Hungary
[2]Department of Inorganic and Analytical Chemistry, Budapest University of Technology and Economics, Budapest H-1111, Hungary

ABSTRACT: ABSTRACT Melt electrospinning (MES) was used to prepare fast dissolving fibrous drug delivery systems in the presence of plasticizers. This new method was found promising in the field of pharmaceutical formulation because it combines the advantages of melt extrusion and solvent-based electrospinning. Lowering of the process temperature was performed using plasticizers in order to avoid undesired thermal degradation. Carvedilol (CAR), a poorly water-soluble and thermal-sensitive model drug, was introduced into an amorphous methacrylate terpolymer matrix, Eudragit® E, suitable for fiber formation. Three plasticizers (triacetin, Tween® 80, and polyethylene glycol 1500) were tested, all of which lowered the process temperature effectively. Scanning electron microscopy, X-ray diffraction, differential scanning calorimetry, and Raman microspectrometry investigations showed that crystalline CAR turned into an amorphous form during processing and preserved it for longer time. *In vitro* dissolution studies revealed ultrafast drug dissolution of the fibrous samples. According to the HPLC impurity tests, the reduced stability of CAR under conditions applied without plasticizer could be avoided using plasticizers, whereas storage tests also indicated the importance of optimizing the process parameters during MES.
Keywords: melt electrospinning; extrusion; amorphous; solid dispersion; enhanced dissolution rate; oral drug delivery; viscosity; plasticizer; HPLC ; Raman spectroscopy

INTRODUCTION

Melt electrospinning (MES) is a promising new technique to prepare fibrous drug-loaded polymer-based solid dispersions for drug delivery systems with controlled release properties. The importance of oral dosage forms with enhanced drug dissolution is increasing as there are a growing number of active pharmaceutical ingredients (API) with poor water solubility, thus, with insufficient bioavailability[1,2] while the oral route of administration is the most convenient for the patients.[3,4]

There are diverse methods to prepare drug-loaded solid dispersions using polymers and other excipients meeting the requirements of the pharmaceutical industry.[5–13] One of these methods is the melt extrusion, a solvent-free continuous tool for dispersing API in a polymeric matrix, thereby improving its dissolution.[14–17] The pharmaceutical viability of melt extrusion is proven by marketed products (Kaletra, Isoptin SR-E) as well.[18]

Another technique offering unique capabilities is electrospinning, a fiber production process using the drawing force of electrostatic field to produce nanofibers from a viscous solution of a polymer and the API. The achievable fast dissolution of the drug substance stems from the amorphous structure accompanied with high surface area of the fibrous mat consisting of hydrophilic polymer carrier,[19] as it derives from the Noyes–Whitney equation.[20] Besides enteral drug formulations,[21–25] solvent-based electrospinning has been used to elaborate tissue engineering scaffolds,[26] wound dressings,[27] implants,[28] and transdermal drug delivery systems[29] as well.

Despite of the various applications, a relatively low number of articles can be found describing a solvent-free implementation of electrospinning (MES). In turn, the lack of solvent has numerous advantages. All the steps of the technology related with the solvent as well as those devices can be omitted, such as dissolving the polymer, tail gas cleaning, and explosion-proof design. Consequently, the technology becomes not only simpler, greener, and safer but economically more reasonable. Moreover, the risk of toxic solvent residue in the fibers can be eliminated making MES a preferred technique for tissue engineering[30–32] and oral drug delivery purposes. The fusion of melt extrusion and MES can be a feasible continuous scaled-up industrial process.[33,34] Thus, coupling with MES, melt extrusion can acquire the unique feature, which solvent-based electrospinning natively owns, that solid dispersions with high surface area can be produced in one single step. Moreover, the fast cooling of the fibers can overcome a limitation of the melting methods, the undesired recrystallization of the drug substance.

The studies about MES are dealing with mostly water-insoluble thermoplastic polymers having limited pharmaceutical importance.[35–40] In most of these cases, high temperatures were necessary to lower viscosity and achieve fiber formation (considering the inverse relationship between temperature and melt viscosity). Therefore, the high temperature can be considered as one of the main drawbacks of MES. Addition of plasticiz-

ers to the polymer can resolve this difficulty thereby preventing the melt from being thermally degraded. Plasticizers are generally used in the plastics industry to improve certain mechanical properties.[41] Since wide choice of polymers have found their way into the pharmaceutical industry, plasticizers became an important modifying agent in drug formulations.[41–43] Despite the obvious benefits of plasticizers, only a few articles reported this strategy while using MES.[44, 45]

In our recent study, we have demonstrated the first example regarding the applicability of MES to prepare drug-loaded hydrophilic polymer fibers with ultrafast drug dissolution.[46] However, despite the strong plasticizing effect of the molecularly dissolved API, the MES process could be performed at a relatively high temperature. The main limitation of the melting methods for preparation of solid dispersions is that the heat-labile drug components can decompose at higher process temperatures,[47, 48] which is of a great importance from the viewpoint of regulations regarding pharmaceutical impurities.[49]

Thus, in this work, we investigated the feasibility of different plasticizers to lower the process temperatures of the applied melt methods, extrusion, and MES. The plasticizers used [Triacetin (TA), Tween® 80 (TW), and polyethylene glycol 1500 (PEG 1500)] are referred to as United States Food and Drug Administration approved inactive pharmaceutical ingredients. Our primary aims were to evaluate the thermal effects of MES on the API and to improve the dissolution of a model drug, carvedilol (CAR). Furthermore, storage tests were performed in respect of chemical and physical stability of the API.

MATERIALS AND METHODS

Materials

Carvedilol (Fig. 1a) from Sigma–Aldrich (Budapest, Hungary) with purity ≥99% was used as API. The melting point of CAR is 117°C.[17] Eudragit® E PO (EPO; Fig. 1b) was kindly provided by Evonik (Darmstadt, Germany), which is a butylmethacrylate-(2-dimethylaminoethyl)-methachrylate-methylmethacrylate amorphous copolymer (1:2:1), with an average molecular weight of 47 kDa. Three different types of plasticizers were used as additives from Sigma–Aldrich, TA (purity: ≥98%), TW (purity: ≥98%), and PEG (average molecular weight: 1500 Da).

Melt Extrusion

Extrudates containing CAR were prepared by HAAKE Mini-Lab micro compounder (Thermo-Haake, Karlsruhe, Germany) to feed the MES equipment. A certain amount of EPO and CAR (20%) was mixed well with and without different types and concentrations of plasticizers. The mixture was introduced into the hopper of the mini extruder. The rotation speed was fixed at 50 rpm, the temperature was 130°C without plasticizer and 100°C with plasticizer content. A compressed flat tablet with a diameter of about 13 mm and a thickness of 0.5 mm (Camilla OL95; Manfredi, Torino, Italy) was prepared from the unplasticized extruded composition for the dissolution tests.

Melt Electrospinning

The previously prepared melt extruded solid dispersions were fed into MES equipment, which was designed and built at Department of Organic Chemistry, Budapest University of Technology and Economics (Budapest, Hungary). The MES equip-
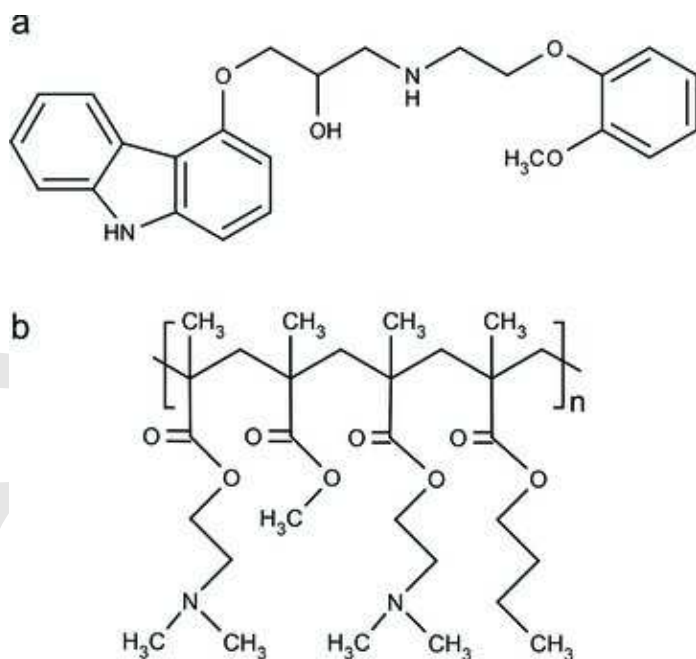

Figure 1. Formula of (a) carvedilol and (b) Eudragit® E.

ment (Fig. 2) has two temperature controlled zones and a programmable feeder. The applied feeding rate was 1 mL/h, the feeding temperatures (T_B) were similar to that of melt extrusion. Needle temperature (T_A) was experimentally determined at given feeding rate by increasing the temperature gradually. The distance of the spinneret and the collector was 10 cm. The stainless steel metal syringe is easy to clean, the needle part is dismountable, and the capillary tube can be replaced for a new experiment, if it is needed.

Differential Scanning Calorimetry

Differential scanning calorimetry (DSC) measurements were carried out using a TA Instruments Q2000 DSC apparatus (New Castle, Delaware) (sample weight: ∼2–3 mg, closed aluminum pan, 50 mL/min nitrogen purge gas). The temperature program consisted of an isothermal period, which lasted for 1 min at −30°C, with subsequent linear heating from −30°C to 200°C at the rate of 10°C/min.

Scanning Electron Microscopy

Morphology of the samples was investigated by a JEOL 6380LVa (JEOL, Tokyo, Japan) type scanning electron microscope (SEM). Each specimen was fixed by conductive double-sided carbon adhesive tape and sputter coated with gold prior to the examination. Applied accelerating voltage and working distance were 15 kV and 10 mm, respectively.

X-Ray Diffraction

Powder X-ray diffraction (XRD) patterns were recorded by a PANanalytical X'pert Pro MDP X-ray diffractometer (Almelo, The Netherlands) using Cu-Kα radiation (1.542 Å) and Ni filter. The applied voltage was 40 kV, whereas the current was 30 mA. The untreated materials, physical mixture (mixed in a mortar by a pestle), and extrudates were analyzed for angles 2θ between 4° and 42°.
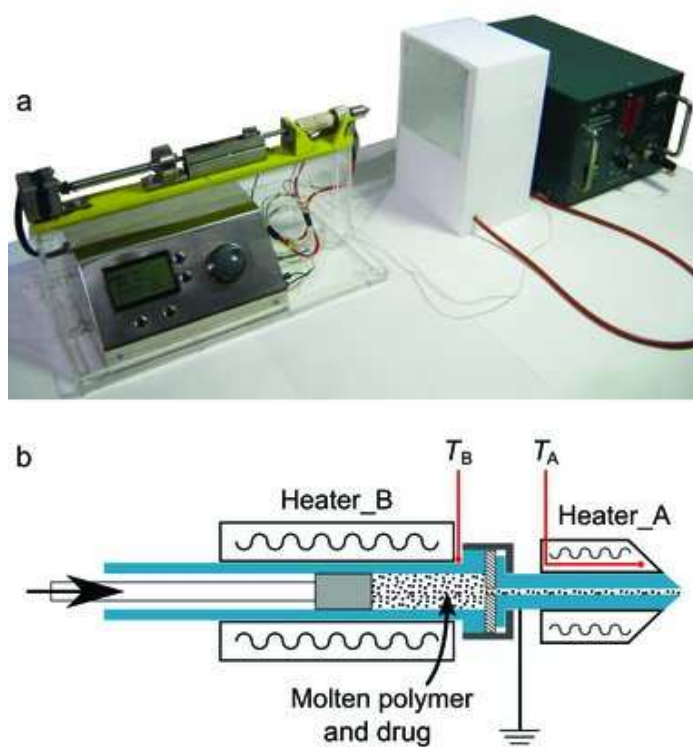
Figure 2. The photograph of the melt electrospinning apparatus (a) and the drawing of the two-zone-heated stainless steel metal syringe (b).

Rheology

Viscosity measurements as a function of temperature were carried out of the extruded samples using an AR 2000 Rotational Rheometer (TA Instruments) in oscillating mode with a parallel plate configuration. The upper moved portion was a 40 mm diameter steel plate and the lower portion was a Teflon-coated Peltier plate. The extruded samples were placed on the preheated Peltier plate and melted. The upper plate was then lowered to the gap of 500 µm. The controlled variable was the oscillating torque, oscillatory tests were carried out at torques of 10, 100, and 1000 µNm at 1 Hz frequency, but no significant changes were detected as a function of torque, dynamic stress sweep tests confirmed that the measurements were made in the linear viscoelastic region. The temperature was ramped down from 170°C to 110°C with a linear rate of 5°C/min. The tests were carried out in triplicate.

Raman Microscopy

Raman mapping was carried out using a Horiba Jobin–Yvon LabRAM (Longjumeau, France) system coupled with an external diode laser source (785 nm, 80 mW) and an Olympus BX-40 optical microscope. The extruded samples were cut carefully to obtain a flat surface and mapped with an objective of 100× magnification in order to investigate the homogeneity and the physical state of the incorporated API. The measured area was $25 \times 25\ \mu m^2$ in all cases. The component concentrations were estimated with the classical least squares (CLSs) method using the reference spectra of the pure components collected on the same device under the same conditions. Visualized score maps were created with LabSpec 5.41 (Horiba Jobin–Yvon).

HPLC Studies

Chemical stability of CAR during the formulation process and a storage period was determined through analyzing the decomposition byproducts using RP-HPLC (Agilent 1200 series LC System; Santa Clara, California). A gradient elution of 0.1 M phosphoric acid and acetonitrile was performed at a flow rate of 1.0 mL/min and 25°C, the UV detection wavelength was set to 285 nm (Agilent 1200 series Diode Array Detector). Fifty milligrams of the extruded and melt electrospun samples was dissolved in the initial mobile phase of gradient elution (0.1 M phosphoric acid/acetonitrile = 60/40, v/v%) obtaining a 1 mg/mL solution of CAR, 20 µL of this stock solution was injected onto the column [Thermo Scientific™ BDS Hypersil C18 column (5 µm; $250 \times 4.6\ mm^2$); Waltham, Massachusetts]. The amount of the degradation products was determined based on the peak areas. The absorption coefficients of the byproducts are higher than that of the pure CAR,[50] which precludes the underestimation of the concentration of the degradation products. The chromatography tests were performed in duplicate.

In Vitro Dissolution Measurement

The dissolution studies were performed using an Erweka DT6 dissolution tester (USP II apparatus, Heusenstamm, Germany). Samples equivalent to 12.5 mg of CAR were added directly in the dissolution vessel containing 900 mL 0.1 M HCl maintained at $37 \pm 0.5°C$ and stirred at 100 rpm. Samples (5 mL) were collected periodically and the concentration of CAR was determined by UV spectrophotometry at 242 nm (Hewlett-Packard HP 8452A; Palo Alto, California) using a diode array detector at 242 nm. Percentage of dissolution was readily calculated according to the calibration curves of CAR in 0.1 M HCl because of the lack of absorption peaks of EPO and the plasticizers in this range.

RESULTS AND DISCUSSION

Process Optimization

For the reduction of applied temperatures of the preparation of extruded and melt electrospun products, different plasticizers were selected and added to the mixture of CAR and the polymer. Factors to be taken into consideration during plasticizer selection were water solubility, compatibility with the EPO matrix, and molecular weight. To minimize the dissolution time of API, the additive has to be freely soluble in water. The classical plasticizers used for ammoniated methacrylate ester copolymers like EPO are low molecular weight esters (glycerol esters, citrate esters).[43] One of these esters used in this study is TA with good water solubility ($M_w = 218$ Da). Plasticizers with higher molecular weight were used as well as to investigate the impact of plasticizing effectiveness on the MES process. Thus, TW, an amphiphile sorbitan ester ($M_w = 1310$ Da), and PEG 1500 were tested. At ambient temperature, TW is a viscous liquid, whereas PEG 1500 is a crystalline solid with melting temperature of approximately 40°C, above which its viscosity is low becoming promising candidate as a plasticizer.

Extrudates were prepared with 20% CAR and with two different concentrations of the chosen plasticizers, 5% and 10%, respectively. Because of the presence of the additive, the extrusion temperatures could be decreased notably, and it was fixed generally to 100°C, except the unplasticized dispersion (see Ta-
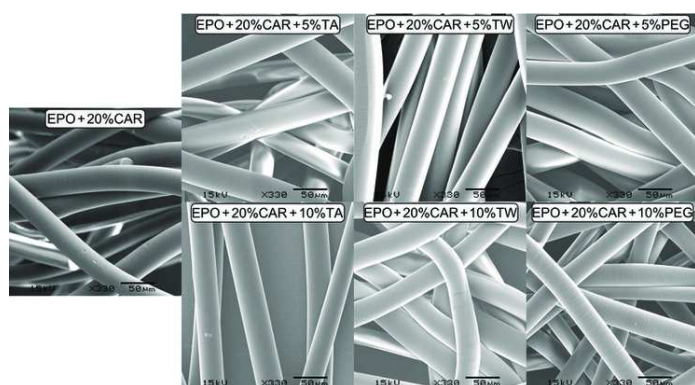
Figure 3. Scanning electron microscopic images of Eudragit® E-based melt electrospun fibers containing 20% carvedilol with and without different plasticizers [triacetin (TA), Tween® 80 (TW), PEG 1500 (PEG)].

ble 1). The extrudates of EPO and CAR in combination with TA and TW were yellowish transparent, whereas the extrudate obtained with PEG was white opaque.

Melt electrospinning method was systematically optimized for each composition and carried out using the extrudate samples as feedstock material. The main goal of optimization was to minimize the degradation product of API in the electrospun fibers. According to this, the fiber formation and feeding temperatures, as well as the melt flow rate were set to the less critical values at which the product morphology remained acceptable. The feeding speed was fixed at a slightly elevated 1.0 mL/h, whereas the appropriate minimum fiber formation temperature was determined by increasing the needle temperature in 5°C steps until the movement of the molten polymer jet became more vigorous, which contributes to the desired reduction in fiber diameter.[35]

Morphology

The obtained fiber morphologies are shown in Figure 3. In spite of the various fiber formation temperature used, the SEM images of the samples show that most of the diameters of the prepared melt electrospun fibers are within a 30–40 μm range in all cases. The likelihood of the occurrence of thicker fibers was small, which implies a typical lognormal diameter distribution.[51] The increased specific surface area of the mats can have the desired accelerating effect on the dissolution time based on the Noyes–Whitney equation.

Rheology

Rheology studies were carried out to find a relationship between the melt viscosity, being the most important technological property of MES, and the minimal heating temperature required for stabile production regime. The results are shown in Figure 4. According to the oscillatory viscosity measurements, the complex viscosity data sets describe well the suitable MES temperatures for each sample composition. The complex viscosity range required for fiber production is around 100–200 Pa s. The viscosity values belonging to the optimized MES temperatures (marked on the diagram for each composition) draw a near horizontal line. This regular behavior of the melt enables a simple prediction method to determine the suitable MES temperature by a rheology measurement for a given type of polymeric
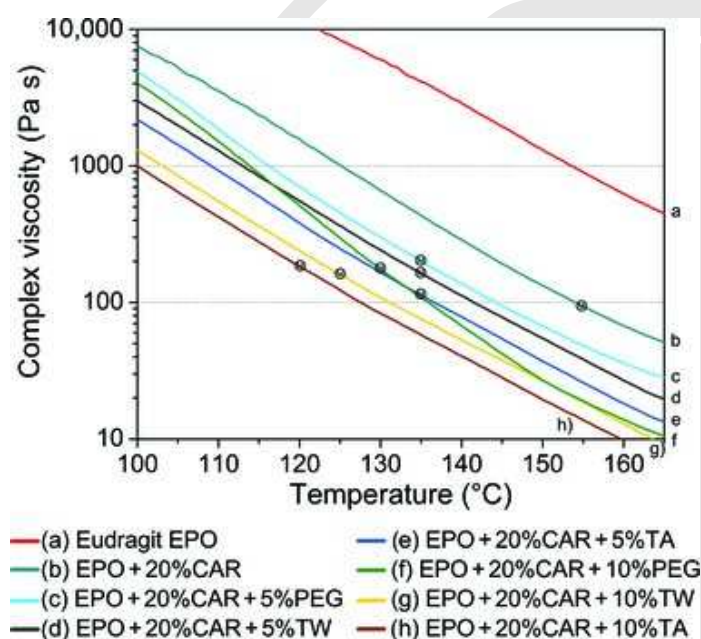
matrix regardless of the other additives. In addition, the repeated oscillatory rheology measurements provide precise and reliable results. The melt viscosity of pure EPO is one order of magnitude larger at all melt temperatures than that of with API (and plasticizer) content. An extrapolation indicates that MES temperature of EPO would be over 180°C, at which, however, a severe decomposition reaction is induced,[52] thus EPO is not convenient for MES as a pure polymer. The addition of CAR alone to the polymer lowered, however, the viscosity dramatically, enabling fiber formation at a reduced 155°C temperature. Further significant viscosity reduction was achieved at plasticizer concentrations of 5%. In these cases, the applied MES temperatures were set to the same value. The plasticizing effectiveness was practically similar for the three plasticizers at this level. Although the curve of the 5%TA sample shows that the MES would be achievable at lower temperatures (∼130°C), it was set also to 135°C in order of the easier evaluation of the experiment results. Plasticizer content of 10% led to additional decrease in melt viscosity and electrospinning temperatures and allowed a better comparison between the additives. TA, of low-molecular weight, exhibited the most efficient plasticizing effect, TW also showed a strong ability in viscosity reduction, the MES temperatures went down to 120°C and 125°C, which are below the extrusion temperature of the EPO + 20%CAR composition. In the case of the PEG-containing samples, the change in melt viscosity was moderate compared with the other two plasticizers. The curves became closely straight after the logarithmic linearization, except the 10%PEG sample (curve f), the viscosity of which curve showed irregular behavior. Above 150°C, the viscosity of EPO + 20%CAR + 10%PEG melt almost exceeds the performance level of the 10%TW sample, however, at lower temperatures both the 5%PEG and 10%PEG curves asymptotically converge to each other. A possible explanation is as follows: the PEG has limited miscibility with the EPO matrix over a certain ratio of plasticizer, nevertheless, the miscibility is greatly improving as the temperature rises.

Differential Scanning Calorimetry

In order to investigate the physical state of API and to evaluate further the plasticizing effect of the additives, DSC measurements were performed (Fig. 5). The physical mixture of 5% crystalline CAR and EPO was analyzed, the curve shows the melting point of CAR at 117°C, and the glass transition of the carrier polymer at 60°C.[46] The thermograms of the melt electrospun fibers did not show the endotherm peak of CAR, which demonstrates the good efficiency of the extrusion–MES tandem process in amorphization of CAR. However, the intensive mixing and shearing process occurs during extrusion rather than at MES suggesting that the main role in amorphization is assigned to the former part of the production line. The lowering of glass transition temperatures of EPO in the presence of different additives indicates the plasticizing effects of these compounds. In the case of the samples containing TA and TW, the T_g of the matrix shifted below the room temperature, whereas the samples with only 20% CAR and with PEG the T_g remained above the room temperature (40°C). The concentration of the plasticizer does not affect the T_g values significantly, only minor shifts can be seen in the thermograms. Nevertheless, if PEG content was increased from 5% to 10%, the T_g value increased too instead of further decrease which may be the consequence of the above-mentioned limited miscibility of PEG and EPO. The melting of a separated crystalline PEG phase can influ-

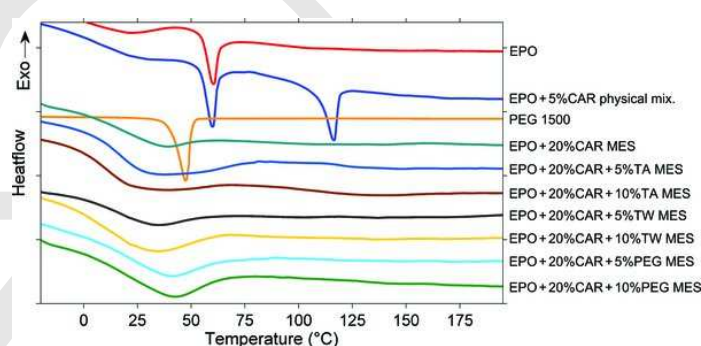**Table 1.** Compositions and Operating Temperatures of the Samples

Sample	CAR (Mass%)	EPO (Mass%)	Plasticizer (Mass%)	Extrusion Temperature (°C)	Extruder Rotation Speed `(rpm)	MES Temperature (°C)	MES Feeding Rate (mL/h)
EPO + 20%CAR	20	80	0%	130	50	155	1
EPO + 20%CAR + 5%TA	20	75	5% Triacetin	100	50	135	1
EPO + 20%CAR + 10%TA	20	70	10% Triacetin	100	50	120	1
EPO + 20%CAR + 5%TW	20	75	5% Tween 80	100	50	135	1
EPO + 20%CAR + 10%TW	20	70	10% Tween 80	100	50	125	1
EPO + 20%CAR + 5%PEG	20	75	5% PEG 1500	100	50	135	1
EPO + 20%CAR + 10%PEG	20	70	10% PEG 1500	100	50	130	1

Figure legend (left):
- (a) Eudragit EPO
- (b) EPO + 20%CAR
- (c) EPO + 20%CAR + 5%PEG
- (d) EPO + 20%CAR + 5%TW
- (e) EPO + 20%CAR + 5%TA
- (f) EPO + 20%CAR + 10%PEG
- (g) EPO + 20%CAR + 10%TW
- (h) EPO + 20%CAR + 10%TA

Figure 4. Complex viscosity of pure Eudragit® E (EPO) and Eudragit® E-based solid dispersions with 20% carvedilol (CAR) and different plasticizers [triacetin (TA), Tween® 80 (TW), PEG 1500 (PEG)] as a function of temperature ($\omega = 1$ Hz).

Figure 5. Differential scanning calorimetry thermograms of the pure Eudragit® E, physical mixture of Eudragit® E and 5% carvedilol, PEG 1500, and the melt electrospun (MES) samples with 20% carvedilol and different plasticizers [triacetin (TA), Tween® 80 (TW), PEG 1500 (PEG)].
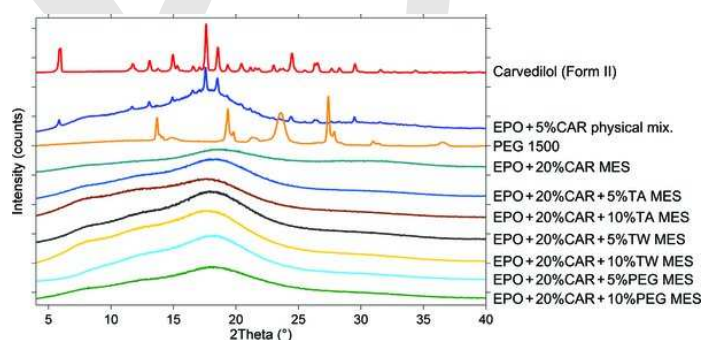
Figure 6. X-ray diffraction patterns of crystalline carvedilol (Form II), physical mixture of Eudragit® E and 5% carvedilol, PEG 1500, and the melt electrospun (MES) fibers with 20% carvedilol and different plasticizers [triacetin (TA), Tween® 80 (TW), PEG 1500 (PEG)].

ence the T_g measurement as the melting point of PEG is near to the peak belonging to the glass transition. Despite suspected limited miscibility and higher MES temperatures, PEG seems to be the most appropriate plasticizer for MES using EPO matrix as the processability of the PEG containing fibers is far better because of their rigidity. Fibrous mats with T_g values below room temperature were hard to handle as their stickiness prevented further processing steps (e.g., grinding) too.

X-Ray Diffraction

A conventional method to investigate crystallinity in solid dispersions is the XRD the result of which is shown in Figure 6. The physical mixture of 5% CAR and EPO served as reference in this case too. The most intense diffraction peaks ($2\theta = 5.9°$, $17.6°$, $18.5°$) of CAR were still observable in the case of the physical mixture, whereas the lack of the peaks suggests that the API and the crystalline excipients turned into an amorphous

form during processing in the MES samples. In the case of PEG content, however, crystalline peaks would be expected to confirm the limited mutual miscibility of semicrystalline PEG and EPO. The lack of diffraction peaks resulting from PEG can also mean that only small volume units exist in a highly ordered state and therefore the broadened peaks are hard to identify.

Physical Stability Testing Using Raman Mapping

Classical analytical methods (XRD, DSC) to investigate crystallinity can be insensitive if only small quantities of crystals
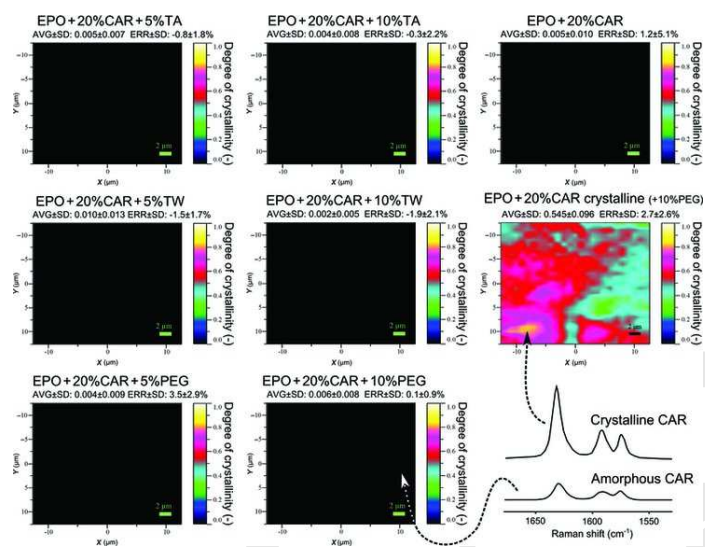
Figure 7. Raman maps illustrating the degree of crystallinity of carvedilol in Eudragit® E-based extrudates (20% carvedilol) with and without different plasticizers [triacetin (TA), Tween® 80 (TW), PEG 1500 (PEG)] after 1 month storage (25°C, 60% RH) and a crystalline reference extrudate (AVG: average degree of crystallinity (-) ± SD, ERR: average error of fit (%) ± SD, $n = 625$).

are distributed in the polymeric matrix. This is the case if crystallinity of an amorphous solid dispersion has to be investigated at an early stage of stability testing. Therefore, Raman mapping was used to detect crystalline API in the samples exposed to room environment [25°C, 60% relative humidity (RH)] for 1 month in open glass bottles, the results can be seen in Figure 7. The results from the aforementioned classical analytical methods (XRD, DSC) did not show any crystallinity regardless the preparation method (extruded and melt electrospun) after 1 month and even in the case of the crystalline reference, a poorly extruded dispersion (EPO + 20%CAR + 10%PEG composition, 10 rpm, 80°C) only weak traces of crystallinity were detectable. According to the Raman measurements, the poorly extruded sample contained a large extent of crystalline CAR, whereas the unplasticized and plasticized samples were amorphous after 1 month. The degree of crystallinity of the API was calculated by CLSs method using the reference spectra of the pure components based on the fact that observable differences appear between the amorphous and the crystalline CAR spectrum. The errors of the CLS fit were averaged for each map, the obtained values indicate that this method can precisely determine the degree of crystallinity, that is, the calculated spectra describe well the measured Raman spectra.

The amorphous CAR spectrum was determined from the mapped spectra as a grand average by a multivariate curve resolution algorithm. A reduced spectral range (1530–1680 cm⁻¹) was found appropriate to perform the degree of crystallinity calculations because in this range the other excipients are not Raman active and there are sharp differences between the spectrum of crystalline and amorphous CAR (shift of peak maximum, change in Raman scattering intensity). The obtained Raman maps clearly demonstrate the difference between the amorphous and crystalline state.

RP-HPLC Studies

A HPLC–UV method was used to analyze the chemical content of the prepared solid dispersions. The aim of the assay was to quantify the possible degradation product of CAR. The results are shown in Table 2, the impurities could be precisely determined according to the small deviations between the repeated measurements. The polymeric matrix and the plasticizers can be considered as thermally stabile compounds used in practice.[43,52,53] In order to differentiate between the thermal effects of extrusion and MES steps, the extrudates and the melt electrospun fibers were measured separately. The current International Conference on Harmonisation guideline of impurities in drug products describes the relevant limits of the degradation products. The absolute maximum dose of CAR is 2×50 mg daily,[54] thus the limits for each degradation products are as follows: reporting threshold—above 0.1%, identification threshold—above 0.2%, qualification threshold—above 200 µg (in this case, it equals to 0.2% as well).[49] As it can be seen in Table 2, the untreated CAR also contained a certain amount of impurities (0.08%), which were far below of any thresholds. It was found during the evaluation that there is a clear correlation between the suffered heat stress and the amount of an impurity, 4-hydroxicarbazole.[50] Directly after the production (day 0), only the EPO + 20%CAR MES sample exceeded the threshold level of 0.2% (0.24% of 4-hydroxycarbazole), which is because of the highest preparation temperature values used in this case. The second largest 4-hydroxycarbazole content belongs to the EPO + 20%CAR extrudate (0.11%). In the case of the samples with plasticizer, none of the impurities exceeded even the reporting threshold, whereas no 4-hydroxycarbazole was detected in the extrudates of those. Comparing the different additives, there were no significant differences in respect of impurities between the extruded and melt electrospun samples if they contained 5% plasticizer. Despite the strongly decreased MES temperature, the most contaminated fibers were those with 10% TA and 10% TW plasticizer, however, this contamination cannot be attributed to 4-hydroxycarbazole and not originated from the plasticizer content according to our additional measurements. This slightly increased chemical instability may be contributed to the lowered viscosity of the carrier, due to ease of molecular movements (increased reactivity) at higher temperature in a more liquid like polymeric matrix.

The HPLC method was used to investigate the chemical stability of the samples over 1 month (25°C, 60% RH, open bottle) as well. The results show similar tendencies compared with the thermal degradation trends, although the differences between the plasticizers became more visible. In this case, however, the 4-hidroxycarbazole content remained the same after the storage test period because of the lack of thermal stress. According to the storage tests, the TA-containing samples were the most degraded systems, more than one percent of the API transformed. The TW showed some protecting effect on the API considering that both TA and TW had a strong plasticizing behavior. As a general trend, the fibers contained more impurities than the extrudates after 1 month, which can be assigned to the increased specific surface area of the mat. Besides this, extrudates and fibers containing PEG were the least degraded systems in respect of thermal degradation and storage tests. In this case, the supramolecular network formed by EPO and PEG linear chains may preserve CAR in its original molecular form. This protecting effect and the improved processability assign

Table 2. Impurity Content Determined with HPLC of Unprocessed Crystalline Carvedilol (CAR), the Prepared Extrudates (Extr), and Melt Electrospun Fibers (MES) Containing 20% Carvedilol and Different Plasticizers [Mean ± SD ($n = 2$)] [(Triacetin (TA), Tween® 80 (TW), PEG 1500 (PEG)]

Sample	Total Impurities (Day 0) (%)	4-Hydroxycarbazole (Day 0) (%)	Total Impurities after 1 Month (%)
Pure carvedilol	0.08 ± 0.00	BDL	0.09 ± 0.00
EPO+20%CAR Extr	0.19 ± 0.01	0.11 ± 0.01	0.21 ± 0.00
EPO + 20%CAR MES	0.34 ± 0.02	0.24 ± 0.02	0.35 ± 0.01
EPO + 20%CAR + 5%TA Extr	0.12 ± 0.00	BDL	0.35 ± 0.01
EPO + 20%CAR + 5%TA MES	0.16 ± 0.01	0.02 ± 0.00	0.41 ± 0.00
EPO + 20%CAR + 10%TA Extr	0.13 ± 0.01	BDL	1.76 ± 0.11
EPO + 20%CAR + 10%TA MES	0.19 ± 0.02	0.01 ± 0.00	2.08 ± 0.10
EPO + 20%CAR + 5%TW Extr	0.10 ± 0.01	BDL	0.17 ± 0.01
EPO + 20%CAR + 5%TW MES	0.14 ± 0.00	0.02 ± 0.00	0.24 ± 0.01
EPO + 20%CAR + 10%TW Extr	0.12 ± 0.01	BDL	0.26 ± 0.01
EPO + 20%CAR + 10%TW MES	0.16 ± 0.01	0.01 ± 0.00	0.32 ± 0.01
EPO + 20%CAR + 5%PEG Extr	0.09 ± 0.01	BDL	0.15 ± 0.01
EPO + 20%CAR + 5%PEG MES	0.13 ± 0.02	0.05 ± 0.02	0.17 ± 0.01
EPO + 20%CAR + 10%PEG Extr	0.08 ± 0.01	BDL	0.17 ± 0.00
EPO + 20%CAR + 10%PEG MES	0.12 ± 0.00	0.04 ± 0.00	0.18 ± 0.01

BDL, below the detection limit.
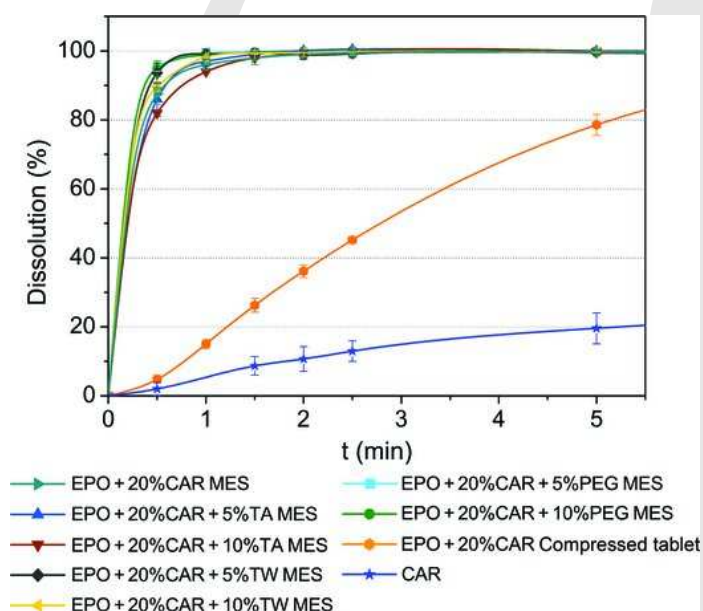
Figure 8. Dissolution profiles of carvedilol (CAR) [12.5 mg dosage, 900 mL 0.1 M HCl, USP Dissolution Apparatus 2 (paddle), 50 rpm, 37°C]. Eudragit® E-based melt electrospun fibers (MES) with 20% carvedilol and different plasticizers [triacetin (TA), Tween® 80 (TW), PEG 1500 (PEG)]; Eudragit® E-based compressed tablet with 20% carvedilol; unprocessed crystalline carvedilol. The error bars indicate the standard deviations ($n = 3$).

PEG a good plasticizer for EPO-based melt electrospun fibers containing a thermosensitive drug. On the basis of the obtained results from HPLC, the strategy of using plasticizers fulfilled the expectations to protect API from thermal degradation and the storage tests revealed the otherwise obvious importance of the correct excipient selection.

In Vitro Dissolution

In vitro studies were carried out to investigate the dissolution properties of the fibers. As it can be seen in Figure 8, significant improvements were achievable compared with the crystalline CAR.

The plasticized and unplasticized samples have very similar ultrafast dissolution characteristic, as the good water solubility of the plasticizers did not affect negatively the drug release kinetics. The fastest drug dissolution belongs to those with PEG additive due to the good fragility during weighing and the consequently outstanding dispersion in the dissolution media. The rapid dissolution of the fibrous samples can be attributed mainly to the following reasons: (1) no need to overcome the crystal lattice energy of API as it is in a thoroughly dispersed amorphous form, thus this significant kinetic barrier is eliminated, (2) the excipients are highly soluble in the acidic dissolution media, moreover there is an accelerating effect through the repulsive Coulomb-forces between the protonated dimethyl-amino side groups of EPO, (3) the formed large specific surface area (according to the Noyes–Whitney equation). In order to uncouple the effect of the increased surface area from the other two facilitating effects, a simple test was carried out. A flat, round shaped tablet was compressed from the EPO + 20%CAR composition, thus the surface area could be neglected. The initial dissolution rate of the compressed tablet was at least one order of magnitude lower than that of the fibrous samples confirming the importance of the increased specific surface area, which in fact is a critic necessary condition. Our previous study has shown that besides the increased surface area, the porosity of a fibrous dosage form is also a dominant factor in the dissolution mechanism[46] because the wettability of rough surfaces (e.g., fibrous grid) strongly depends on the pore structure characteristics.[55]

CONCLUSIONS

Melt electrospinning for preparation of microfibers containing a thermosensitive model drug with poor water solubility was studied. Application of plasticizers effectively decreased the melting temperatures, thus, the degradation of the API content could be hindered too according to the HPLC studies. Oscillatory rheology measurements confirmed the plasticizing effect of the additives and the API itself providing a good way to predict the minimal fiber forming temperature. Processing of the crystalline API in twin-screw extruder, it turned into an amorphous form in all formulations because of the intensive

shear strength of mixing. To overcome the not sufficient sensitivity of DSC and XRD, Raman microspectroscopy was used to determine the degree of crystallinity. The Raman mapping combined with chemometric methods indicated that the API preserved its amorphous form even after 1-month storage in room environment. Comparing the different plasticizers with each other, the PEG showed excellent protection against drug decomposition during processing and storage, while the processibility of the fibers remained still acceptable, which was not the case for the other plasticizers with lower molecular weight. The dissolution experiments revealed ultrafast drug release rate from the fibers, in contrast to the hydrophobic crystalline drug. The novel, optimized solvent-free MES drug formulation technique extends the applicability of solvent-based electrospinning and melt extrusion by combining their advantages (e.g., solvent-free, continuous process, high surface area, effective amorphization).

The major focus in the subsequent work must be placed on the development of new polymeric matrices with pH-independent dissolution.

ACKNOWLEDGMENTS

REFERENCES

1. Keseru GM, Makara GM. 2009. The influence of lead discovery strategies on the properties of drug candidates. Nat Rev Drug Discov 8:203–212.

2. Lipinski CA. 2000. Drug-like properties and the causes of poor solubility and poor permeability. J Pharmacol Toxicol 44:235–249.

3. Sastry SV, Nyshadham JR, Fix JA. 2000. Recent technological advances in oral drug delivery—A review. Pharm Sci Technol Today 3:138–145.

4. Langer R. 1993. Polymer-controlled drug delivery systems. Accounts Chem Res 26:537–542.

5. Vasconcelos T, Sarmento B, Costa P. 2007. Solid dispersions as strategy to improve oral bioavailability of poor water soluble drugs. Drug Discov Today 12:1068–1075.

6. Fülöp Z, Nielsen TT, Larsen KL, Loftsson T. 2013. Dextran-based cyclodextrin polymers: Their solubilising effect and self-association. Carbohyd Polym 97:635–642.

7. Fülöp Z, Gref R, Loftsson T. 2013. A permeation method for detection of self-aggregation of doxorubicin in aqueous environment. Int J Pharm 454:559–561.

8. Szűts A, Lang P, Ambrus R, Kiss L, Deli MA, Szabó-Révész P. 2011. Applicability of sucrose laurate as surfactant in solid dispersions prepared by melt technology. Int J Pharm 410:107–110.

9. Muehlenfeld C, Kann B, Windbergs M, Thommes M. 2013. Solid dispersions prepared by continuous cogrinding in an air jet mill. J Pharm Sci 102:4132–4139.

10. Vajna B, Farkas I, Farkas A, Pataki H, Nagy ZK, Madarasz J, Marosi G. 2011. Characterization of drug–cyclodextrin formulations using Raman mapping and multivariate curve resolution. J Pharm Biomed 56:38–44.

11. Allesø M, Chieng N, Rehder S, Rantanen J, Rades T, Aaltonen J. 2009. Enhanced dissolution rate and synchronized release of drugs in binary systems through formulation: Amorphous naproxen–cimetidine mixtures prepared by mechanical activation. J Control Release 136:45–53.

12. Alonzo DE, Gao Y, Zhou D, Mo H, Zhang GGZ, Taylor LS. 2011. Dissolution and precipitation behavior of amorphous solid dispersions. J Pharm Sci 100:3316–3331.

13. Marsac PJ, Rumondor ACF, Nivens DE, Kestur US, Stanciu L, Taylor LS. 2010. Effect of temperature and moisture on the miscibility of amorphous dispersions of felodipine and poly(vinyl pyrrolidone). J Pharm Sci 99:169–185.

14. Patyi G, Bodis A, Antal I, Vajna B, Nagy ZK, Marosi G. 2012. Thermal and spectroscopic analysis of inclusion complex of spironolactone prepared by evaporation and hot melt methods. J Therm Anal Calorim 102:349–355.

15. Sauceau M, Fages J, Common A, Nikitine C, Rodier E. 2010. New challenges in polymer foaming: A review of extrusion processes assisted by supercritical carbon dioxide. Prog Polym Sci 36:749–766.

16. Thommes M, Kleinebudde P. 2006. Use of κ-carrageenan as alternative pelletisation aid to microcrystalline cellulose in extrusion/spheronisation. I. Influence of type and fraction of filler. Eur J Pharm Biopharm 61:59–67.

17. Nagy ZK, Sauceau M, Nyúl K, Rodier E, Vajna B, Marosi G, Fages J. 2012. Use of supercritical CO_2-aided and conventional melt extrusion for enhancing the dissolution rate of an active pharmaceutical ingredient. Polym Adv Technol 23:909–918.

18. Maniruzzaman M, Boateng JS, Snowden MJ, Douroumis. 2012. A review of Hot-melt extrusion: Process technology to pharmaceutical products. ISRN Pharm 2012.

19. Nagy ZK, Balogh A, Vajna B, Farkas A, Patyi G, Kramarics Á, Marosi G. 2011. Comparison of electrospun and extruded Soluplus®-based solid dosage forms of improved dissolution. J Pharm Sci 101:322–332.

20. Noyes AA, Whitney WR. 1897. The rate of solution of solid substances in their own solutions. J Am Chem Soc 19:930–934.

21. Nagy ZK, Nyúl K, Wagner I, Molnár K, Marosi G. 2010. Electrospun water soluble polymer mat for ultrafast release of Donepezil HCl. Express Polym Lett 4:763–772.

22. Vrbata P, Berka P, Stránská D, Doležal P, Musilová M, Čižinská L. 2013. Electrospun drug loaded membranes for sublingual administration of sumatriptan and naproxen. Int J Pharm 457:168–176.

23. Yu DG, Williams GR, Wang X, Liu XK, Lic HL, Bligh SWA. 2013. Dual drug release nanocomposites prepared using a combination of electrospraying and electrospinning. RSC Adv 3:4652–4658.

24. Yu DG, Liu F, Cui L, Liu ZP, Wang X, Bligh SWA. 2013. Coaxial electrospinning using a concentric teflon spinneret to prepare biphasic-release nanofibers of helicid. RSC Adv 3:17775–17783.

25. Yu DG, Hu MH, Zhou W, Chen BY, Wang X. 2013. Electrospun ketoprofen sustained release nanofibers prepared using coaxial electrospinning. Appl Mech Mater 395:138–143.

26. Rampichová M, Martinová L, Košťáková E, Filová E, Míčková A, Buzgo M, Michálek J, Přádný M, Nečas A, Lukáš D, Amler E. 2012. A simple drug anchoring microfiber scaffold for chondrocyte seeding and proliferation. J Mater Sci Mater Med 23:555–563.

27. Sridhar R, Sundarrajan S, Vanangamudi A, Singh G, Matsuura T, Ramakrishna S. 2013. Green processing mediated novel polyelectrolyte nanofibers and their antimicrobial evaluation. Macromol Mater Eng. [Epub ahead of print.]

28. Ranganath SH, Wang CH. 2008. Biodegradable microfiber implants delivering paclitaxel for post-surgical chemotherapy against malignant glioma. Biomaterials 29:2996–3003.

29. Wu XM, Branford-White CJ, Zhu LM, Chatterton NP, Yu DG. 2010. Ester prodrug-loaded electrospun cellulose acetate fiber mats as transdermal drug delivery systems. J Mater Sci Mater Med 21:2403–2411.

30. Dalton PD, Klinkhammer K, Salber J, Klee D, Möller M. 2006. Direct in vitro electrospinning with polymer melts. Biomacromolecules 7:686–690.

31. Farrugia BL, Brown TD, Upton Z, Hutmacher DW, Dalton PD, Dargaville TR. 2013. Dermal fibroblast infiltration of poly(ε-caprolactone) scaffolds fabricated by melt electrospinning in a direct writing mode.

Biofabrication 5.

32. Bock N, Woodruff MA, Steck R, Hutmacher DW, Farrugia BL, Dargaville TR. 2013. Composites for delivery of therapeutics: Combining melt electrospun scaffolds with loaded electrosprayed microparticles. Macromol Biosci.

33. Lyons J, Li C, Ko F. 2004. Melt-electrospinning part I: Processing and geometric properties. Polymer 45:7597–7603.

34. Malakhov SN, Khomenko AY, Belousov SI, Prazdnichnyi AM, Chvalun SN, Shepelev AD, Budyka AK. 2009. Method of manufacturing nonwovens by electrospinning from polymer melts. Fibre Chem 41:355–359.

35. Zhou H, Green TB, Joo YL. 2006. The thermal effects on electrospinning of polylactic acid melts. Polymer 8:7497–7505.

36. Kim SJ, Jang DH, Park WH, Min BM. 2010. Fabrication and characterization of 3-dimensional PLGA nanofiber/microfiber composite scaffolds. Polymer 51:1320–1327.

37. Dalton PD, Calvet JL, Mourran A, Klee D, Möller M. 2006. Melt electrospinning of poly(ethylene glycol-block-ε-caprolactone). Biotechnol J 1:998–1006.

38. Brown TD, Slotosch A, Thibaudeau L, Taubenberger A, Loessner D, Vaquette C, Dalton PD, Hutmacher DW. 2012. Design and fabrication of tubular scaffolds via direct writing in a melt electrospinning mode. Biointerphases 7:1–16.

39. Mazalevska O, Struszczyk MH, Krucinska I. 2012. Design of vascular prostheses by melt electrospinning—Structural characterizations. J Appl Polym Sci 129:779–792.

40. Wang XF, Huang ZM. 2010. Melt electrospinning of PMMA. Chinese J Polym Sci 28:45–53.

41. Wypych G. 2012. Handbook of plasticizers. 2nd ed. Toronto, Canada: ChemTec Publishing.

42. Crowley MM, Zhang F, Repka MA, Thumma S, Upadhye SB, Battu SK, McGinity JW, Martin C. 2007. Pharmaceutical applications of Hot-melt extrusion: Part I. Drug Dev Ind Pharm 33:909–926.

43. Snejdrova E, Dittrich M. 2012. Pharmaceutical application of plasticized polymers, Recent advances in plasticizers; Luqman M , Ed. Rijeka, Croatia: InTech, pp 69–90.

44. Zhao F, Liu Y, Ding Y, Yan H, Xie P, Yang WM. 2012. Effect of plasticizer and load on melt electrospinning of PLA. Key Eng Mat 501:32–36.

45. Li H, Ding Y, Liu Y, Zhang Y, Yang WM. 2013. The preparation of polypropylene/polyvinyl alcohol ultra-fine fibers using melt electrospinning method. Key Eng Mat 561:8–12..

46. Nagy ZK, Balogh A, Drávavölgyi G, Ferguson J, Pataki H, Vajna B, Marosi G. 2012. Solvent-free melt electrospinning for preparation of fast dissolving drug delivery system and comparison with solvent-based electrospun and melt extruded systems. J Pharm Sci 102:508–517.

47. Thumma S, ElSohly MA, Zhang SQ, Gul W, Repka MA. 2008. Influence of plasticizers on the stability and release of a prodrug of Δ^9-tetrahydocannabinol incorporated in poly (ethylene oxide) matrices. Eur J Pharm Biopharm 70:605–614.

48. Jijun F, Lili Z, Tingting G, Xing T, Haibing H. 2010. Stable nimodipine tablets with high bioavailability containing NM-SD prepared by hot-melt extrusion. Powder Technol 204:214–221.

49. International Conference on Harmonisation. 2006. Note for guidance on impurities in new drug products.

50. Stojanović J, Vladimirovm S, Marinković V, Veličković D, Sibinović P. 2007. Monitoring of the photochemical stability of carvedilol and its degradation product by the RP-HPLC method. J Serb Chem Soc 72:37–44.

51. Gu SY, Ren J, Wu QL. 2005. Preparation and structures of electrospun PAN nanofibers as a precursor of carbon nanofibers. Synthetic Met 155:157–161.

52. Lin SY, Yu HL. 2000. Microscopic Fourier transform infrared/differential scanning calorimetry system used to study the different thermal behaviors of polymethacrylate copolymers of Eudragit RS, RL, E 30D, or E. J Appl Polym Sci 78:829–835.

53. Ghebremeskel AN, Vemavarapu C, Lodaya M. 2006. Use of surfactants as plasticizers in preparing solid dispersions of poorly soluble API: Stability testing of selected solid dispersions. Pharm Res 23:1928–1936.

54. Rickli H, Steiner S, Müller K, Hess OM. 2003. Betablockers in heart failure: Carvedilol safety assessment (CASA 2-trial). Eur J Heart Fail 6:761–768.

55. Grundke K, Bogumil T, Gietzelt T, Jasobasch HJ, Kwok DY, Neumann AW. 1996. Wetting measurements on smooth, rough and porous solid surfaces. Interfaces Surf Colloid Eng 101:58–68.